STM study of the initial stages of AlF_3 on Cu(100)

J. C. Moreno-López,[1,*] R. A. Vidal,[1] M. C. G. Passeggi, Jr.,[1] and J. Ferrón[1,2]

[1]*Laboratorio de Superficies e Interfaces, Instituto de Desarrollo Tecnológico para la Industria Química (CONICET-UNL), Güemes 3450, S3000GLN Santa Fe, Argentina*

[2]*Departamento de Materiales, Facultad de Ingeniería Química, Universidad Nacional del Litoral, Santiago del Estero 2829, S3000AOM Santa Fe, Argentina*

(Received 25 September 2009; revised manuscript received 30 November 2009; published 17 February 2010)

In this study we present results concerning the early growth stages of an insulator-metal interface by means of scanning tunneling microscopy. We report the growth of aluminum fluoride (AlF_3) films over a Cu(100) surface at room temperature, from submonolayer coverages up to 1.25 monolayers. Scanning tunneling microscopy (STM) measurements reveal that aluminum fluoride islands undergo a shape transition at very low coverages, from compact to fractal-like, as they grow in size. These fractal-like islands cover the substrate with a single monolayer film up to depositions of 0.80 monolayers, while for larger coverages the growth results in the formation of three dimension islands. Kinetic Monte Carlo simulations help us to understand some issues of the growth mechanism. High voltages ($V \geq 2.50$ V) are needed to obtain STM images, showing the insulator character of the AlF_3 islands.

DOI: 10.1103/PhysRevB.81.075420 PACS number(s): 68.55.aj, 68.43.Jk, 68.37.Ef

I. INTRODUCTION

The composition, growth mechanism and structure of thin films of insulators deposited on several metal surfaces are topics that have attracted widespread interest in recent years. Work in this field has been motivated by the quality requirements of thin films needed to develop advanced microelectronic, optical, and magnetic devices, as well as nanometer-scale structures.[1] Recently, there is a growing interest in the use of ultrathin insulating layers, grown over metallic surfaces, to hold up nanostructures with the aim of decoupling their electronic states from those of the substrate and to reduce charging effects,[2] e.g., in the assembly of organic molecules on ultrathin insulators,[3] and in the study of the interactions between spins in linear chains of Mn atoms on CuN islands,[4] among others.

Growth studies typically involve depositions of a controlled amount of atoms, or molecules, onto a well-characterized crystalline substrate at prescribed growing conditions. The deposition of atoms onto a substrate is a nonequilibrium process; the system tries to restore equilibrium by forming aggregates. The ad-atoms migrate on the surface and when meeting each other they can form critical nuclei, which subsequently can grow by attachment of further ad-atoms. Nucleation of new islands and growth of existing islands are competing processes. As coverage increases, the islands density increases until the critical nucleation density is reached. In this steady-stage regime, newly deposited atoms will predominantly join existing islands and effectively prevent nucleation of new islands.[1]

In order to understand the growth of insulators on metals some important efforts based on scanning tunneling microscopy (STM) have been made. Recently, Sun *et al.*[2] have studied NaCl multilayer islands grown on Au(111)-$(22\times\sqrt{3})$. Changing the tunneling parameters they were able to selectively image atomically resolved NaCl islands or the gold reconstruction below the first NaCl layer. Calleja *et al.*[5] showed the epitaxial growth of CaF_2 on Cu(111) as a function of deposition temperature and coverage, reporting from their observations the epitaxial growth of twinned CaF_2(111) crystallites on Cu(111). Farías *et al.*[6] found that the upper and lower side of the step edges act as nucleation centers in the low temperature growth of LiF molecules on Ag(111), suggesting that this nucleation mechanism in principle should be also present in the growth of other insulator-on-metal systems at low temperatures. On the other hand, Fölsch *et al.*[7] showed selective NaCl growth on Cu(211), creating alternative stripes of bare Cu and NaCl-covered areas, and Bertrams and Neddermeyer,[8] reported the growth of NiO(100) layers on Ag(100), studied as a function of coverage and annealing.

Insulator layers of aluminum fluoride (AlF_3) are of particular interest for their potential applications in nanometer-scale patterning through electron beam lithography,[9–14] due to that under electron irradiation they show radiolysis, i.e., the desorption of the fluoride with the consequent formation of an aluminum metallic layer.[14–17] Sánchez *et al.*,[18] reported a layer-by-layer (LbL) growth of AlF_3 thin films on Al(111) surfaces by means of Auger electron spectroscopy (AES) and electron energy loss spectroscopy (EELS). Vergara *et al.*,[13] characterized the growth process of AlF_3 films on GaAs(110) from submonolayer coverages up to several layers, by means of AES, ion sputter depth profiling and direct recoiling spectroscopy with time of flight analysis (TOF-DRS).

In thin-film growth, as islands start to develop specific island morphologies or shapes arise. The existence of fractal islands has been reported essentially only on triangular lattice geometry. In contrast, growth on square lattice geometry has so far always resulted in compact islands. These observations have been explained through the higher barrier of edge diffusion on triangular and hexagonal lattices, due to an ad-atom has to lower its coordination when crossing a corner.[1] However, Müller *et al.*[19] reported the growth of fractal Cu islands over a square Ni(100) lattice, explaining this behavior on the basis of the strain relief in heteroepitaxial islands.

In our work, we report a scanning tunneling microscopy (STM) study of the initial growth stages of AlF_3 on Cu(100) at room temperature, showing an island shape transition from compact to fractal, similar to the observed by Müller *et al.*[19] However, we have reproduced the experimental results by considering only shadowing effects and a large mobility of the AlF_3 molecules using kinetic Monte Carlo (KMC) simulations. Some important features, such as the shape transition and the growth of smaller islands close to the steps can be understood in fact on the basis of our simple KMC simulations. The synergism between STM measurements and KMC simulations has tremendously improved our understanding of the kinetic aspects of the AlF_3 on Cu(100) growth.

II. EXPERIMENTAL SETUP AND SIMULATIONS

All STM measurements were carried out at room temperature in an ultra-high-vacuum (UHV) chamber, with a base pressure in the low 10^{-10} mbar range. The Cu(100) substrate was cleaned in a reaction chamber attached to the main UHV chamber, by cycles of Ar^+ ion bombardment followed by annealing at 900 K. The temperature was measured by means of a chromel-alumel thermocouple attached to the backside of the sample holder.

The aluminum fluoride films were deposited "*in situ*" onto the Cu(100) at room temperature (300 K) using a Knudsen cell mounted in the reaction chamber, charged with anhydrous AlF_3 (CERAC INC., Milwaukee, Wisconsin, USA, 99.5%) and heated at 820 K. The cell was carefully degassed and shuttered to avoid sample contamination. Vacuum conditions in the reaction chamber were in the low 10^{-8} mbar range, even throughout the evaporations. It is important to remark that STM images of the clean Cu(100) substrate and AlF_3/Cu(100) samples showed no evidence of contamination after a typical experiment (2–8 h). The deposition rate of AlF_3 was varied between 2×10^{-2} to 8×10^{-4} ML/s. The reported coverages were determined from a direct analysis of the STM images for coverages under 0.80 ML, and by using the evaporation rate assuming a constant sticking coefficient, for coverages beyond 0.80 ML.

Electrochemical etched tungsten tips were used for all STM experiments reported in this work. The polycrystalline W tips were routinely cleaned by Ar^+ ion bombardment and annealing in UHV. All the STM images obtained in this study were acquired in the constant current mode with a sample bias voltages of +2.50 V, with the only exception of an atomic resolution image, and tunneling currents ranging between 0.1–0.6 nA. Acquisition and image processing were performed using the WS×M free software.[20]

The Monte Carlo simulation used in this work is a quite simple one. Our model is a variant of the classical DLA model,[21,22] whose initial state is a seed molecule(s) over a square 2D lattice. A second molecule is added at some random site on the lattice. This particle walks randomly until it visits a site adjacent to the seed, depending on the number of "neighbors" of this site, the molecule can incorporate to the cluster or continue its random walk. We can vary the number of neighbors (considering as neighbors the first and second nearest atoms) needed to freeze a moving molecule from one

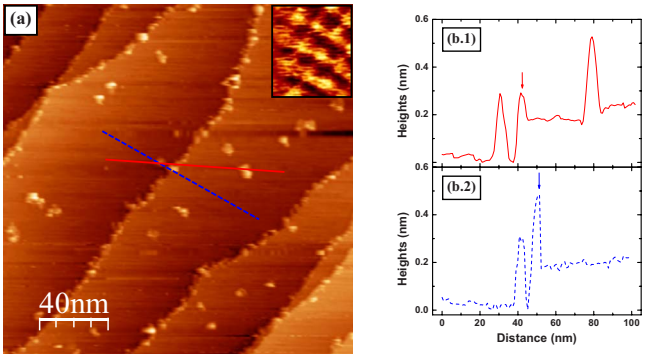

FIG. 1. (Color online) (a) STM image (200×200 nm^2) recorded after the deposition of 0.05 ML of AlF_3 on Cu(100) at 300 K. The image was acquired with a sample bias voltage of V_S=+2.50 V and a tunnel current of I_t=0.1 nA. The inset of figure (a) shows a STM image (0.8×0.9 nm^2) recorded between the AlF_3 islands displaying atomic resolution on Cu(100), with the following tunneling conditions: V_S=+0.02 V and I_t=1 nA. (b) Typical scan profiles acquired along the lines depicted in (a) showing islands nucleated on the lower and upper side of the step-edge, (b.1) and (b.2), respectively.

["hit and stick" DLA (Refs. 21 and 22)] to three atoms (critical number of neighbors). Larger number of neighbors needed to freeze a molecule is incompatible with a square array. It is clear that the binding energy is somehow proportional to the number of near neighbors. In our simulation, we model this situation in an extreme way: below the critical number of neighbors the molecule is free to move (E_b=0), and above it the molecule is frozen (E_b=∞). We assume an infinite diffusion length, i.e., adsorbed molecules move freely over the surface until they reach either a critical nucleus or a step (whenever we have steps). Only after the adsorbed molecule nucleates (on a step or in an existing island) another molecule is adsorbed on the surface. This condition resembles either low evaporation rates (according to our experiments), or high substrate temperatures.

As we will see, the fast decoration of steps observed in the experiments suggests that the actual situation is not so far from our simulation. However, our intention is not to simulate the growth but to test some simple ideas about it. For instance, the nucleation of new islands is not possible within this model, i.e., nucleation centers (seed molecules) must be added at the beginning. However, general trends, like the effect of shadowing paths by the already formed islands (like in DLA system) can be explored.

III. RESULTS AND DISCUSSION

In order to study the initial growth stages of AlF_3 on Cu(100) at room temperature, we performed a STM study as a function of coverage. In Fig. 1(a), we show the surface morphology after the deposition of 0.05 ML of AlF_3. At this stage the step edges of the substrate are completely decorated by islands and only a few have nucleated on the terraces, indicating a rather high diffusion in order to promote migration of AlF_3 molecules to step and kink sites. In the inset of Fig. 1(a), we show an atomically resolved image of the

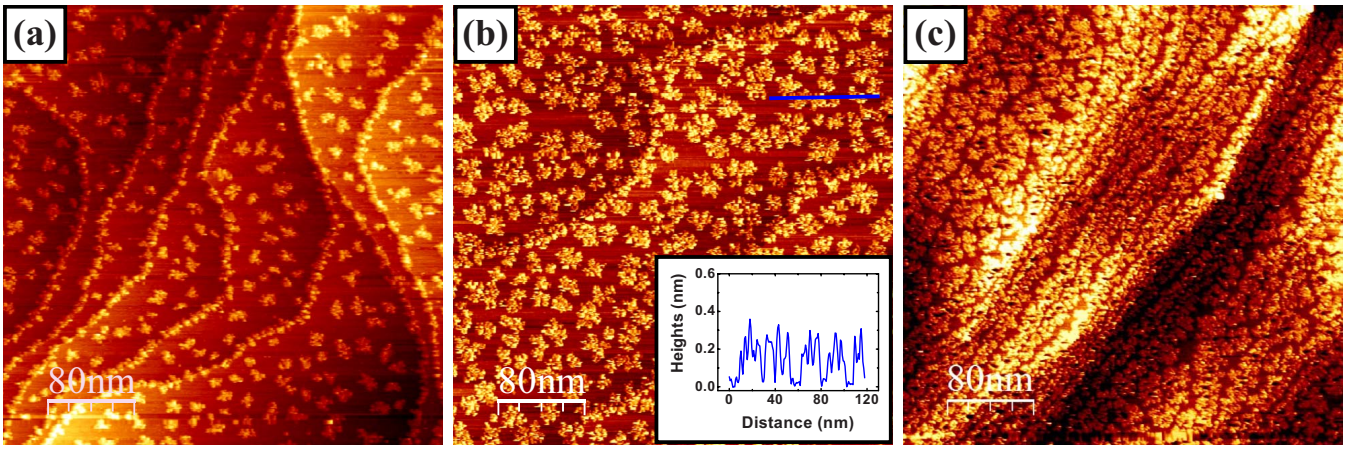

FIG. 2. (Color online) STM images (400×400 nm^2) of AlF_3 deposited on Cu(100) at 300 K, (a) 0.25 ML, (b) 0.50 ML, and (c) 1.10 ML. The images were acquired at $V_S=+2.50$ V and $I_t=0.10-0.15$ nA. The inset shows the scan profile acquired along the line depicted in (b).

Cu(100) surface recorded between the AlF_3 islands. The atomically resolved image was acquired at a low tunneling voltage of 0.02 V. A square lattice with a nearest-neighbor distance of 0.26 nm is observed, characteristic of the atomic arrangement of the Cu(100) surface.

The apparent height of the AlF_3 islands is about 0.25–0.30 nm, as it is shown in the scan profiles of Fig. 1(b). The difference between the island and the Cu step heights in the very early stages of growth allows us to identify the nucleation site at the step, i.e., lower or upper side. In Fig. 1(b), we show islands nucleated on the lower (b.1) and upper (b.2) side of a step edge. From further analysis of several line profiles we concluded that nucleation of AlF_3 on Cu(100) at step edges proceeds in a rather symmetrical way, i.e., the nucleation probability is almost the same for AlF_3 molecules approaching a step from the upper or lower terraces. Farías *et al.*[6] have reported a similar growth mechanism at step edges for LiF on Ag(111), explaining their results through a localized charge redistribution at step sides, which favors adsorption of polar molecules on both the upper and lower sides of the step edges. These results show a clear difference with metal on metal growth, where nucleation is preferentially located at the lower step side.[23–26]

The AlF_3 islands deposited on Cu(100) are imaged using relatively high positive sample bias voltages, e.g., injecting electrons in the conduction band of AlF_3, indicating the insulating character of the film. No images could be acquired with negative bias voltages. For sample bias voltages lower than +2.50 V the islands are frequently swept away by the tip during the scanning showing typical STM images of a "clean" Cu(100) surface suggesting that AlF_3 molecules are adsorbed over the surface without a chemical reaction with the copper atoms.

In Fig. 2, we show a series of STM images revealing the evolution of the AlF_3 islands with increasing coverage. We observe that new islands nucleate on the terraces and grow laterally (2D) developing a fractal-like shape. In Fig. 2(a), we show a STM image of the surface after the deposition of 0.25 ML of AlF_3 on Cu(100). At this stage the density of islands on the terraces is 1.4×10^{11} islands per cm^2, the average distance between first neighbors is 16.7 nm, and the islands height are between 0.25–0.30 nm, i.e., one monolayer high.

In Fig. 2(b), we show a STM image of the surface after the deposition of 0.50 ML of AlF_3 on Cu(100). At this stage the islands height are still between 0.25–0.30 nm, as we can observe in the scan profile showed in the inset, the density of island nucleated on the terraces and the average distance between first neighbors remain constant, 1.5×10^{11} island per cm^2 and 16.9 nm, respectively. The constant density of islands with increasing coverage indicates that the critical nucleation density has already been achieved at 0.25 ML.

An ad-molecule landed on the surface undergoes a random walk and has two alternatives that determine its fate: (1) the ad-molecule may find an existing island and incorporate to it leading to growth, or (2) it may find one or more other diffusing ad-molecules to nucleate forming a new island. When the critical nucleation density has been achieved, 0.25 ML in our case, newly deposited molecules will predominantly join existing islands and effectively prevent nucleation of new islands. In consequence, in this steady-stage regime the probability for an ad-molecule to find one or more other diffusing ad-molecules nucleating in a new island is practically zero. Therefore, for narrow terraces (width less than the distance between two islands at 0.25 ML, ~17 nm) the probability to nucleate an island on it is practically zero, and a step-flow regime is expected, as effectively occurs in the step bunches regions with terraces width less than 17 nm.

A careful observation of Fig. 2(b), tells us that the AlF_3 islands grow at both sides of the step edges, as we have already pointed out, and also shows that step-edge islands grow at a slower rate than terrace islands. Once the islands density on the terraces has reached its stationary value, i.e., the distance between islands is below the ad-molecules diffusion length, the increase in the islands size will depend on the local island density. Since around the steps the island density is larger than on the terraces, it is obvious that islands located at the step edges will grow at a slower rate, reaching smaller sizes, as it is clearly shown in Fig. 2(b).

With further deposition, the coverage also increases and the islands grow laterally covering the substrate with a single

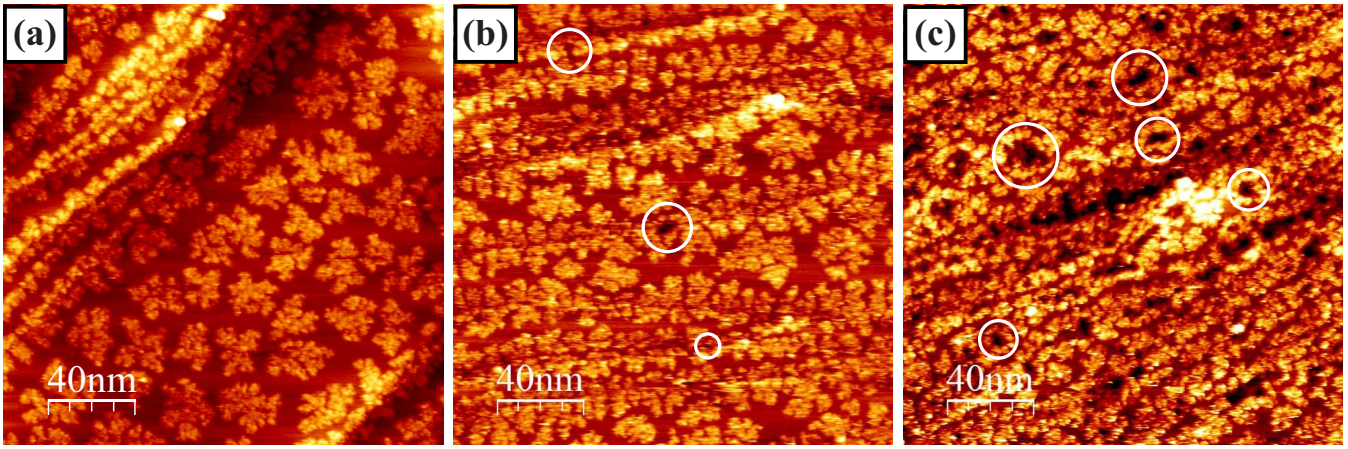

FIG. 3. (Color online) STM images (200×200 nm^2) of AlF_3 deposited on Cu(100) at 300 K, (a) 0.75 ML, (b) 0.85 ML, and (c) 1.25 ML, showing a clear evolution of the dark areas with further depositions of AlF_3. As a guide for the eyes we have marked some of the dark areas with circles in (b) and (c). The images were acquired at V_S=+2.50 V and I_t=0.10–0.15 nA.

monolayer (2D film), even up to coverages as large as 0.80 ML. Therefore, all molecules deposited (before 0.80 ML) on top of the islands can reach the island edges and go down until nucleation of a new layer occurs on top of an island. A molecule landing on top of an island may find a higher potential-energy barrier as it attempts to hop off the island to the lower layer, this additional barrier exists because an atom reduces its coordination while it crosses the island edge,[1] this is the so-called Ehrlich-Schwoebel barrier.[27,28] Therefore, the 2D growth until 0.80 ML indicates that the AlF_3 molecules landed on top of existing islands have a sufficient diffusion length in order to reach the island edges and a relatively small Ehrlich-Schwoebel barrier.[27,28]

In Fig. 2(c), we show an STM image of the surface after the deposition of 1.10 ML of AlF_3 on Cu(100). At this stage, the covered surface area is 80 % and an important number of black patches appear over some islands covering 15 % of the surface. Taking into account that STM images contain both geometrical and electronic information and the insulator character of the AlF_3, we interpret these dark areas as bilayer or even thicker islands of AlF_3. Thus, for coverages larger than 0.80 ML we have that a 3D growth starts. This interpretation is supported by the increase of the dark areas observed for further depositions of AlF_3. In Fig. 3 we show images acquired at coverages from 0.75 to 1.25 ML, where the increase of these dark areas is apparent. We could not acquire STM images beyond 1.25 ML. It is important to be noticed that, in Fig. 3(c) where we show the surface after the deposition of 1.25 ML of AlF_3 on Cu(100), the black patches cover 25 % of the surface. Taking this into account, and the fact that for a deposition of 1.10 ML only 15 % of the surface is covered by black patches, we cannot dismiss the possibility of an important decrease of the sticking coefficient beyond 0.80 ML, i.e., when AlF_3 on AlF_3 growth begins.

Along the AlF_3 growth, at very low coverages an important feature appears concerning the shape of the islands, this is a transition from a compact to a fractal-like form, Fig. 1(a) to Figs. 2(a)–2(c), respectively. In order to understand this transition, in Fig. 4 we show a series of STM images revealing the evolution of the islands shape during the early stages of growth. At the very beginning of the growth the AlF_3 islands are exclusively compact. Further evaporation leads to an increase of the islands size, with a fixed separation between them. However, the growth mode seems to be a bit more complicated than the simple aggregation of diffusing molecules to fixed islands. In Fig. 4(b), the bigger islands appear as to be formed by clusters of rather similar smaller islands. This picture is repeated for increasing coverages, 0.30 ML [Fig. 4(c)], even up to 0.70 ML [Fig. 4(d)]. Large islands seem as formed by an aggregation of small compact islands whose sizes are lower than a critical size ($A_c\sim2.5$ nm, that corresponds to ~100 molecules of the

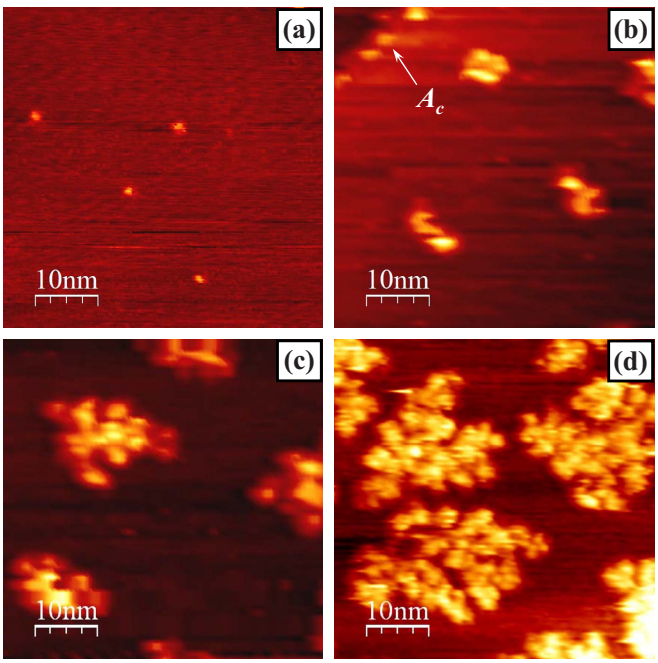

FIG. 4. (Color online) STM images (50×50 nm^2) of AlF_3 deposited on Cu(100) at 300 K, (a) 0.02 ML, (b) 0.05 ML, (c) 0.30 ML, and (d) 0.70 ML. In (b) we have marked an island of critical size, A_c. The images were acquired at V_S=+2.50 V and I_t=0.10–0.15 nA.

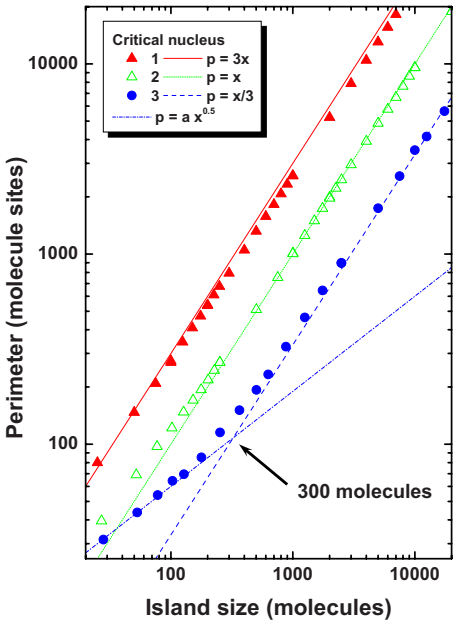

FIG. 5. (Color online) Perimeter evolution vs island size for different binding energy models. The lines are a guide for the eyes, they are not fittings. In the legend, "p" is the perimeter, "x" the island size, and "a" a constant.

stable perovskite-like form of AlF_3, referred usually as α-AlF_3.[29,30] As the size of the islands increases their shapes become more irregular, showing a fractal-like (randomly ramified) shape, Figs. 4(c) and 4(d).

A similar shape transition, from compact to randomly ramified islands, has been observed by Müller *et al.*[19] for Cu on Ni(100). They explained this behavior on the basis of the

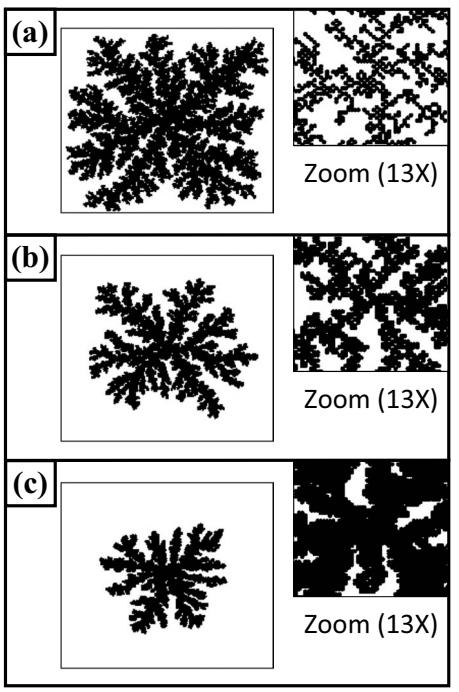

FIG. 6. Snapshots of KMC simulations performed for critical nucleus: (a) 1; (b) 2; (c) 3. The insets show a 13× zoom of the islands. The points size agrees with the zoom.

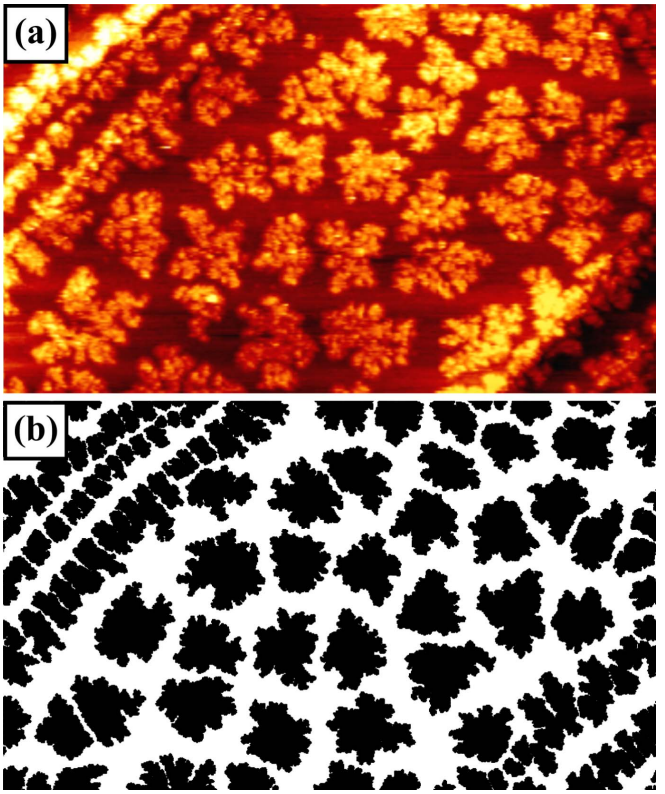

FIG. 7. (Color online) (a) STM images (200×120 nm^2) of 0.75 ML of AlF_3 deposited on Cu(100) at 300 K. The image was acquired at V_S=+2.50 V and I_t=0.1 nA. (b) Simulated kinetic Monte Carlo surface image, using as initial nucleation centers the center points of the islands displayed in (a).

compressive strain in the Cu islands due to the positive lattice mismatch of the two metals (+2.58%). This kind of shape transition was already theoretically predicted by Tersoff and Tromp.[31] As well, Müller *et al.*[19] proposed the evolution of the island perimeter as a relevant parameter to support the idea of an island shape transition. They showed a change in the evolution of the perimeter slope at the very beginning of the growth. However, is the strain the only way of explaining a shape transition as the observed in both cases, i.e., Cu on Ni(100) and AlF_3 on Cu(100)?

In Fig. 5, we show results for the perimeter evolution of the islands coming from our KMC simulations. As we explained above, these simulations are purely kinetic, i.e., neither misfit stress,[31] nor long range (elastic) forces are present. The only changing parameter for the different curves is the number of neighbors needed to freeze the evolving molecule, from one ("hit and stick" DLA,[21,22]) to three neighbor atoms (first and second nearest neighbors). The perimeter slopes show an almost linear dependence with island size for critical nucleus 1 and 2, while in the case of nucleus 3 the linear dependence accounts only for island sizes over a critical value. Below this critical size a clear deviation from this behavior is observed, instead of been linear the dependence goes with the square root of the island size. So, it is clear that a shape transition occurs for islands of about 300 molecules, if the molecules are allowed to have certain mobility around the island edge once nucleated, and this transition has only a geometric origin.

In Fig. 6, we show some snapshots of the different MC simulations that may help up to understand the reason of the slope change and shape transition observed in the perimeter evolution. As we expect, the characteristic arms of the dendritic growth are thicker if we allow the mobility of ad-molecules along the islands edges. However, the main point here is the time needed to develop such arms. In fact, for large islands the shape is quite the same, with different arm thicknesses for the three critical sizes, justifying the same perimeter evolution dependence, i.e., linear with a different slope. However, the development of dendritic arms is delayed for critical nucleus 2 and 3, by the larger ad-molecules mobility around the island edge (see the insets in Fig. 6).

The next step would be to simulate a situation closer to the experimental one where several islands coexists on the terraces and steps growing simultaneously, and competing to capture adsorbed molecules. In Fig. 7, we show a KMC evolution started from an experimental configuration. Since our KMC evolution needs an initial distribution of nucleation centers we obtained them from the central points of the islands.

The agreement between the experimental results and the simulation is quite nice. The KMC simulation resembles the entire main experimental features of the AlF_3 film, including the smaller islands at the steps. The growth of smaller islands close to the steps has also a kinetic origin, i.e., this increased shadowing effect is motivated by the larger island density around steps. As we assumed before, the effect of having simultaneous growing islands, located at distances smaller than the diffusion path of the molecules cuts the developing of the dendritic arms. As we have shown above, most of the features characterizing the growth of AlF_3 can be understood on the basis of a large and limited mobility of AlF_3 molecules on terraces and at the islands edges, respectively.

IV. CONCLUSIONS

We have studied the initial growth stages of AlF_3 on Cu(100) at room temperature, by means of scanning tunneling microscopy and kinetic Monte Carlo simulations. We have shown that at the initial growth stages the AlF_3 molecules completely decorate both sides of the substrate step edges. Around coverages of 0.05 ML, the terraces islands display a shape evolution from a compact to a fractal-like form by a clustering of islands of critical size A_c ($\sim$2.5 nm). Upon further evaporation a lateral 2D film covers the substrate with a single monolayer until 0.80 ML, changing with further deposition to a 3D islands growth mode. By means of kinetic Monte Carlo simulation, we showed that most of the growth features can be understood on the basis of kinetic and geometric factors, i.e., the terraces islands grow faster than the step-edges ones motivated by the larger island density around steps.

ACKNOWLEDGMENTS

This work was financially supported by CONICET, UNL, and ANPCyT through projects PIP Grant No. 5277; CAI+D's Grants No. 2005-02-12 and No. 12-H419; and PICT's Grants No. 2003-12-14730 and 2006-01138; respectively.

*Corresponding author. FAX: +54 (342) 455-0944; jcmorenolopez@intec.unl.edu.ar

[1] Z. Zhang and M. G. Lagally, Science **276**, 377 (1997).
[2] X. Sun, M. P. Felicissimo, P. Rudolf, and F. Silly, Nanotechnology **19**, 495307 (2008).
[3] L. Ramoino, M. von Arx, S. Shintke, A. Baratoff, H.-J. Güntherodt, and T. A. Jung, Chem. Phys. Lett. **417**, 22 (2006).
[4] C. F. Hirjibehedin, C. P. Lutz, and A. J. Heinrich, Science **312**, 1021 (2006).
[5] F. Calleja, J. J. Hinarejos, A. L. Vázquez de Parga, S. M. Suturin, N. S. Sokolov, and R. Miranda, Surf. Sci. **582**, 14 (2005).
[6] D. Farías, K.-F. Braun, S. Fölsch, G. Meyer, and K. H. Rieder, Surf. Sci. Lett. **470**, L93 (2000).
[7] S. Fölsch, A. Helms, S. Zöphel, J. Repp, G. Meyer, and K. H. Rieder, Phys. Rev. Lett. **84**, 123 (2000).
[8] Th. Bertrams and H. Neddermeyerer, J. Vac. Sci. Technol. B **14**, 1141 (1996).
[9] A. Murray, M. Scheinfein, M. Isaacson, and I. Adesida, J. Vac. Sci. Technol. B **3**, 367 (1985).
[10] G. S. Chen, J. Vac. Sci. Technol. A **17**, 403 (1999).
[11] W. Langheinrich, B. Spangenberg, and H. Beneking, J. Vac. Sci. Technol. B **10**, 2868 (1992).
[12] H. Watanabe, J. Fujita, Y. Ochiai, S. Matsui, and M. Ichikawa, Jpn. J. Appl. Phys., Part 1 **34**, 6950 (1995).
[13] L. I. Vergara, R. A. Vidal, J. Ferrón, E. A. Sánchez, and O. Grizzi, Surf. Sci. **482-485**, 854 (2001).
[14] L. I. Vergara, R. A. Vidal, and J. Ferrón, Appl. Surf. Sci. **229**, 301 (2004).
[15] A. Murray, M. Isaacson, I. Adesida, Appl. Phys. Lett. **45**, 589 (1984).
[16] V. I. Nikolaichik, Philos. Mag. A **68**, 227 (1993).
[17] G. S. Chen and C. J. Humpheys, J. Vac. Sci. Technol. B **15**, 1954 (1997).
[18] E. A. Sánchez, G. Otero, N. Tognalli, O. Grizzi, and V. H. Ponce, Nucl. Instrum. Methods Phys. Res. B **203**, 41 (2003).
[19] B. Müller, L. Nedelmann, B. Fischer, H. Brune, J. V. Barth, and K. Kern, Phys. Rev. Lett. **80**, 2642 (1998).
[20] I. Horcas, R. Fernandez, J. M. Gomez-Rodriguez, J. Colchero, J. Gomez-Herrero, and A. M. Baro, Rev. Sci. Instrum. **78**, 013705 (2007).
[21] T. A. Witten and L. M. Sander, Phys. Rev. Lett. **47**, 1400 (1981).
[22] P. Meakin, Phys. Rev. A **27**, 1495 (1983).
[23] R. Q. Hwang, J. Schröder, C. Günther, and R. J. Behm, Phys. Rev. Lett. **67**, 3279 (1991).
[24] H. Brune, C. Romainczyk, H. Röder, and K. Kern, Nature (London) **369**, 469 (1994).
[25] G. L. Kellogg, Surf. Sci. Rep. **21**, 1 (1994).
[26] J. J. de Miguel, Surf. Rev. Lett. **4**, 353 (1997).
[27] G. Ehrlich and F. G. Hudda, J. Chem. Phys. **44**, 1039 (1966).
[28] R. L. Schwoebel and E. J. Shipsey, J. Appl. Phys. **37**, 3682

(1966).
[29] P. Daniel, A. Bulou, M. Rousseau, J. Nouet, J. L. Fourquet, M. Leblanc, and R. Burriel, J. Phys.: Condens. Matter **2**, 5663 (1990).
[30] A. Le Bail and F. Calvayrac, J. Solid State Chem. **179**, 3159 (2006).
[31] J. Tersoff and R. M. Tromp, Phys. Rev. Lett. **70**, 2782 (1993).